THE ASTROPHYSICAL JOURNAL, 446:826–831, 1995 June 20

DISCOVERY OF THE 18.7 SECOND ACCRETING X-RAY PULSAR GRO J1948+32

DEEPTO CHAKRABARTY,[1] TOWSIAN KOH, LARS BILDSTEN,[2] AND THOMAS A. PRINCE
Division of Physics, Mathematics, and Astronomy, California Institute of Technology, Pasadena, CA 91125

AND

MARK H. FINGER,[3] ROBERT B. WILSON, GEOFFREY N. PENDLETON,[4] AND BRADLEY C. RUBIN[3]
Space Science Laboratory, NASA/Marshall Space Flight Center, Huntsville, AL 35812
Received 1994 August 23; accepted 1994 December 27

ABSTRACT

We have detected an 18.7 s accreting X-ray pulsar in the Cygnus region, using the BATSE large-area detectors on the *Compton Gamma Ray Observatory*. GRO J1948+32 has been localized to within 10 deg^2 using a method we developed for positioning weak pulsed sources with BATSE. During the 33 day outburst, the phase-averaged 20–75 keV pulsed flux rose from 25 mCrab to 50 mCrab over 10 days and then decayed below our detection threshold over nearly 25 days. A photon spectral index of $\gamma = 2.65 \pm 0.15$ (assuming photon flux density $dN/dE \propto E^{-\gamma}$) was measured during a bright interval. The observed modulation of the neutron star's pulse frequency is suggestive of orbital variation over less than one orbit cycle. Assuming a constant spin frequency derivative over the outburst, we can place the following individual 95% confidence limits on each of the pulsar parameters: orbital period $35^d < P_{orb} < 70^d$; orbital radius 75 lt-sec $< a_x \sin i < 300$ lt-sec, eccentricity $e < 0.25$, spin frequency derivative 5×10^{-13} Hz s$^{-1} < \dot{\nu} < 2.5 \times 10^{-11}$ Hz s^{-1}, X-ray mass function $0.5\ M_\odot < f_x(M) < 5\ M_\odot$. As the stellar type of the mass-providing companion is still not known for this source, we briefly speculate on the nature of mass transfer in this system.

Subject headings: pulsars: individual: (GRO J1948+32) — pulsars: individual: (GRO J2014+34) — X-rays: stars

1. INTRODUCTION

Since the discovery of pulsations from Centaurus X-3 over 20 yr ago (Giacconi et al. 1971), more than 30 accretion-powered X-ray pulsars have been detected (see Nagase 1989). Nearly half of these pulsars are transient sources which were discovered during bright outbursts. However, due to incomplete and nonuniform sky coverage, the population and recurrence history of these transients is poorly determined. The Burst and Transient Source Experiment (BATSE) on the *Compton Gamma Ray Observatory* (*GRO*) has provided a nearly continuous all-sky monitor of pulsed hard X-ray ($\gtrsim$20 keV) emission since its launch in 1991 April (Prince et al. 1994). On 1994 April 6 BATSE first detected 18.7 s pulsed hard X-ray emission from a previously unknown source in the Cygnus region of the Galactic plane (Finger et al. 1994). The source was detected at energies as high as 75 keV and reached phase-averaged pulsed intensities $\approx$50 mCrab[5] in the 20–75 keV band during the 33 day outburst. BATSE data taken prior to 1994 April fail to show any pulsed emission near 18.7 s from this region of the sky, indicating that the new source is transient or at least highly variable.

In this paper, we present a detailed analysis of the BATSE observations of GRO J1948+32 as well as a refined estimate (10 deg^2 solid angle with 99% confidence) for its position. The approximate Galactic coordinates of the source are $l \sim 65°$, $b \sim 2°$. A preliminary position estimate for the source (originally designated GRO J2014+34) yielded a 68% confidence error circle with 8° radius, corresponding to a solid angle of 200 deg^2 (Finger et al. 1994). Further observations yielded an improved position with a 90% confidence error box covering a solid angle of 15 deg^2 and led to a redesignation of the source as GRO J1948+32 (Chakrabarty et al. 1994). A preliminary search of the brightest sources in this region in archival data from the *ROSAT*/PSPC soft X-ray (0.1–2.4 keV) all-sky survey failed to detect any pulsed sources with a similar pulse period (Kahabka et al. 1994). A 6° × 6° optical *R*-band plate of the region was obtained during the X-ray outburst, using the Palomar Observatory 1.2 m Oschin Schmidt telescope (I. N. Reid 1994, private communication). Comparison of the 10 deg^2 source error box on this plate with archival plates from the Palomar sky survey (Reid et al. 1990) may aid in the identification of the optical companion.

2. OBSERVATIONS AND ANALYSIS

BATSE is an all-sky monitor of 20 keV–1.8 MeV γ-ray flux (see Fishman et al. 1989 for a description). Our standard detection and timing analysis uses the 20–60 keV channel of the 1.024 s resolution DISCLA data type (Chakrabarty et al. 1993). GRO J1948+32 was initially detected in a routine search of the Fourier power spectra of these data for 1994 April 7. Once the source was discovered, a systematic search of the entire BATSE DISCLA data archive from 1991 April 22 to 1994 November 9 (MJD 48369–49665) was made. The Fourier power spectrum of the data for each day (optimized for the

[1] deepto@srl.caltech.edu.
[2] Current address: Department of Physics and Department of Astronomy, University of California, Berkeley, CA 94720.
[3] Universities Space Research Association.
[4] Department of Physics, University of Alabama, Huntsville, AL 35899.
[5] It is often convenient in X-ray and γ-ray astronomy to refer the photon flux in a given bandpass to a known fiducial, the total emission of the Crab Nebula in the same bandpass. In this usage, 1 Crab $\approx \int_{E_{lo}}^{E_{hi}} 10E^{-2.15}\,dE$ photons cm^{-2} s^{-1}, where photon energy is measured in keV. The Crab is also sometimes used as a fiducial for flux *density* in a bandpass. These usages are equivalent for Crab-like spectra. Both comparisons are of limited utility for spectral shapes dissimilar to the Crab.

source direction) was searched for a statistically significant pulsed signal with a pulse period in the range 18.6 s $\leq P_{\rm pulse} \leq$ 18.8 s. The only detections were during the outburst, from 1994 April 6 to May 12 (MJD 49448–49482). The detection threshold for this analysis was $\approx$25 mCrab (20–60 keV).

For those days where a significant signal was detected in the DISCLA data, the CONT data (20 keV–2 MeV count rates, in 16 energy channels at 2.048 s resolution) were also analyzed. The raw data were preprocessed using the orbital background and bright source occultation model developed by Rubin et al. (1993). Pulse profiles for each of the 16 channels in the background-subtracted CONT data were generated from 2 day folds of the time series corresponding to the outburst. Only data from the detector with the smallest viewing angle to the source were used.

In order to simplify estimation of the measurement uncertainties, we used a single-harmonic model for the pulse to obtain phase-averaged pulsed-component count rates from these pulse profiles. For GRO J1948+32, a single-harmonic model systematically underestimates the pulsed intensity by 25%, due to the small but significant nonsinusoidal component of the pulse shape. We corrected all of the measured pulsed count rates for this factor. Goodman (1985) gives the probability distribution $p(a \mid s, n)$ for the measured harmonic amplitude a given a signal amplitude s and noise strength n. We used Bayes's theorem to invert this function to obtain the probability distribution $p(s \mid a, n)$ for the signal amplitude, allowing an estimate of the pulsed count rate in a noisy pulse profile.[6] These count rates are well fitted by assuming a power-law photon spectrum of the form $dN/dE = C_{30}(E/30\ \text{keV})^{-\gamma}$ and accounting for the BATSE instrumental response. Fluxes for the individual channels are obtained by folding the best-fit values of C_{30} and γ through the BATSE instrumental response. (See Heindl et al. 1993 for a detailed discussion of the procedure for converting count rates to fluxes.) The unpulsed flux of GRO J1948+32 was too faint ($\lesssim$100 mCrab) to be detected using the standard Earth occultation technique described by Harmon et al. (1993).

All the 2 day folds of the background-subtracted CONT data over the outburst yielded statistically significant pulsed flux detections in channels 1–4 (approximately 20–75 keV), and several folds yielded detections in channel 5 (approximately 75–100 keV). Figure 1 shows the 20–75 keV pulsed flux history of the outburst. (If significant channel 5 contributions were to be included in this plot for the appropriate segments, the quoted fluxes would change by less than 10%.) The pulsed flux increased from $(2.2 \pm 0.5) \times 10^{-10}$ ergs cm^{-2} s^{-1} to $(4.9 \pm 0.5) \times 10^{-10}$ ergs cm^{-2} s^{-1} over 10 days before decaying to the minimum detectable level over 25 days. The photon spectral index for these 2 day fits had a mean value $\langle\gamma\rangle = 2.29 \pm 0.08$, with individual values varying between 1.25 ± 0.35 and 2.82 ± 0.39. There was not a statistically significant correlation of the spectral index with either time or pulsed intensity.

[6] We assumed a prior probability $p(s)$ = constant; see de Jager (1994) for a discussion of the strengths and weaknesses of this choice. For $a \gg n$, $p(s \mid a, n)$ is approximately a Gaussian centered at $s = a$ with an associated 1 σ error defined by the symmetrical 68% confidence interval of the distribution. In this case, the computed flux is not sensitive to the choice of prior, and the Bayesian result is identical to that obtained with other methods commonly employed at high signal-to-noise. However for $a \lesssim n$, the distribution is highly skewed and peaks near $s = 0$. In such cases, we quoted a 2 σ upper limit $s_{\rm ul}$ on the count rate, implicitly defined by $\int_0^{s_{\rm ul}} p(s \mid a, n) ds = 0.95$.

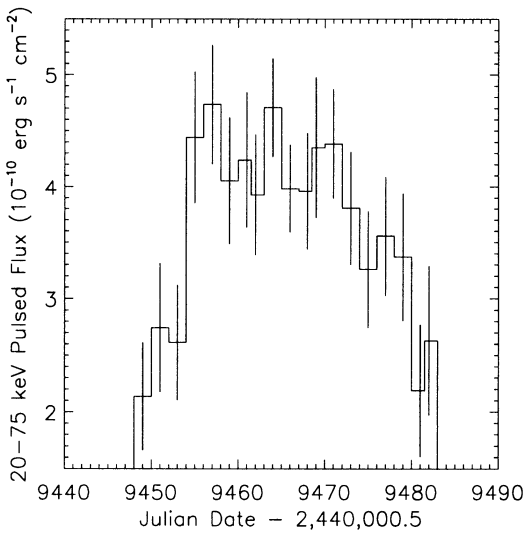

FIG. 1.—Pulse-phase-averaged 20–75 keV pulsed flux history of GRO J1948+32. The vertical bars show the 1 σ uncertainties in the flux measurements.

It is advantageous to phase-connect longer intervals of data in order to probe the high-energy spectrum of the source. However, as the spacecraft orientation of *GRO* is changed (which happens at $\sim$10 day intervals), different detectors will have the best source viewing angle. Because the effective area of the BATSE detectors is a very sensitive function of energy and viewing angle in the 20–100 keV range and since each detector has slightly different energy channel edges, it is difficult to produce count spectra from data combined over more than one pointing. There were three different *GRO* pointings during the outburst, each with a different best viewing angle to the source: 22°.8 for detector 7 on MJD 49448–49461, 3°.6 for detector 0 on MJD 49462–49468, and 26° for detector 6 on MJD 49468–49482. There was no statistically significant change in the source spectral index during these three pointings. Figure 2 shows the measured spectrum during the bright pointing with the most favorable viewing angle, MJD 49462–49468. The left panel shows the measured pulsed count spectrum from a 7 day fold across this interval, and the right panel shows the inferred source photon spectrum assuming a power-law spectral model. In determining upper limits for the flux in the higher channels, no assumption was made about the phase relationship with the pulsed component in the lower channels. The pulse profiles for this interval as a function of energy are shown in Figure 3. For display purposes, these profiles are about twice-overresolved. The best-fit 20–120 keV power-law spectral parameters for the phase-averaged pulsed component during this interval are $\gamma = 2.65 \pm 0.15$ and $C_{30} = (3.4 \pm 0.2) \times 10^{-4}$ photons cm^{-2} s^{-1} keV^{-1}.

The crosses in Figure 4 denote the pulse frequency history observed by BATSE. The quasi-sinusoidal variation may be due to orbital motion of the source; if so, a complete orbital cycle has not yet been observed. Consequently, it is not possible to reliably decouple orbital effects from variations in the intrinsic spin period due to accretion torques, and the orbital parameter estimates remain highly correlated. A wide range of degenerate solutions exist which provide a good fit to the data (solid curve in Fig. 5). However, it is possible to constrain the allowed parameter space. If we assume a circular orbit and a constant spin frequency derivative, then the following 95%

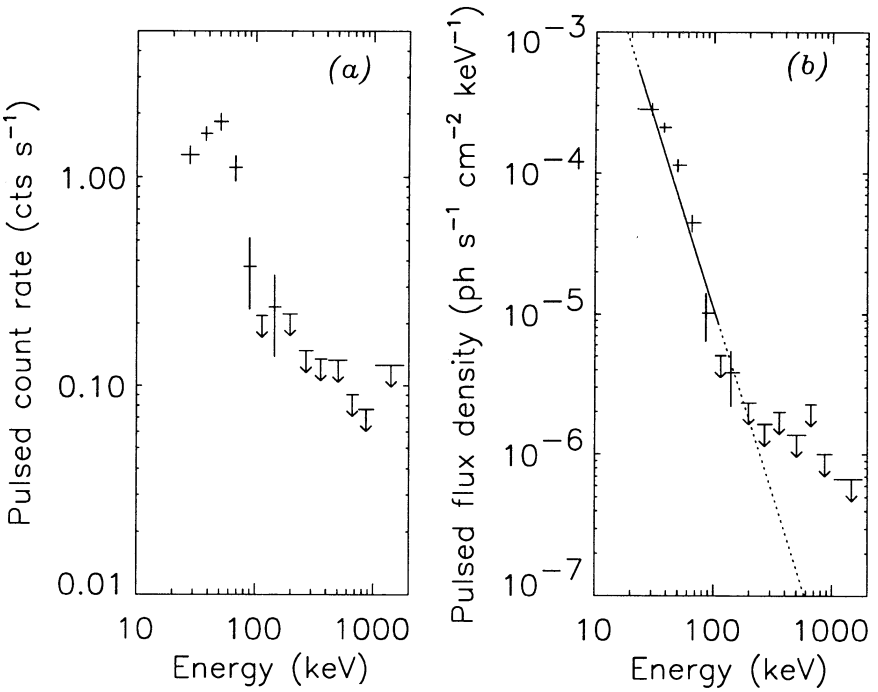

FIG. 2.—(*a*) The phase-averaged pulsed count rate spectrum of GRO J1948+32 for MJD 49462–49468, measured with BATSE large-area detector 0. The viewing angle to the source was 3°. The vertical bars show the 1 σ statistical uncertainties, while the horizontal bars show the widths of the energy channels. Upper limits are quoted at 95% confidence. (*b*) The corresponding phase-averaged pulsed photon spectrum, corrected for the BATSE instrumental response and the source viewing angle. The solid line shows the best-fit power law photon spectral model ($\gamma = 2.65$, $C_{30} = 3.4 \times 10^{-4}$ photons cm^{-2} s^{-1} keV^{-1}).

confidence limits can be placed: orbital period $35^{d} < P_{orb} < 44^{d}$; orbital radius 95 lt-sec $< a_x \sin i <$ 165 lt-sec; spin frequency derivative 2×10^{-12} Hz s$^{-1} < \dot{\nu} < 6 \times 10^{-12}$ Hz s^{-1}, X-ray mass function 0.7 $M_\odot < f_x(M) < 2.3\ M_\odot$. If we permit eccentric solutions, the allowed 95% confidence parameter ranges are broader: eccentricity $e < 0.25$; orbital period $35^{d} < P_{orb} < 70^{d}$; orbital radius 75 lt-sec $< a_x \sin i <$ 300 lt-sec; spin frequency derivative 5×10^{-13} Hz s$^{-1} < \dot{\nu} < 2.5 \times 10^{-11}$ Hz s^{-1}; X-ray mass function 0.5 $M_\odot < f_x(M) < 5\ M_\odot$. It should be noted that these ranges are the individual confidence regions for each of the parameters separately, computed by allowing all the other parameters to vary.

A revised position estimate for GRO J1948+32 was made using the method described in the Appendix with the 20–60 keV DISCLA data for MJD 49448–49482. The frequency, amplitude, and phase of the pulsed signal were assumed constant for each day but were allowed to vary from day to day. We computed the likelihood function for an 8° × 12° grid of positions, spaced by 0°.5 and centered at an earlier position estimate (Chakrabarty et al. 1994). The formal confidence contours were calculated by interpolation between the grid points. These are shown in Figure 5, along with the earlier estimate by Chakrabarty et al. (1994) for comparison.

3. DISCUSSION

GRO J1948+32 is certainly a neutron star; the lower limit on the spin frequence derivative exceeds, by an order of magnitude, the maximum possible spin-up rate for a white dwarf pulsar (6×10^{-14} Hz s^{-1} for accretion at the Eddington critical rate, assuming radius $R_x = 10^9$ cm, mass $M_x = 1.4\ M_\odot$, and spin period $P_{spin} = 18.7$ s). If we assume steady spin-up over the outburst duration, we can further exploit our lower limit on $\dot{\nu}$ to infer that the total X-ray luminosity $L_x \gtrsim 10^{36}$ ergs s^{-1} (Chakrabarty et al. 1993). The upper limit on $\dot{\nu}$, which is within a factor of 3 of the maximum spin-up rate for a neutron star (6×10^{-11} Hz s^{-1} assuming $R_x = 10^6$ cm, $M_x = 1.4\ M_\odot$, and $P_{spin} = 18.7$ s), corresponds to $L_x \lesssim 8 \times 10^{37}$ ergs s^{-1}. Since we have no measure of the bolometric X-ray flux, we are unable to place useful limits on the distance to the source.

The nature of the mass transfer in this system is not clear. The values of P_{spin} and P_{orb} are consistent with the correlation generally observed in Be/X-ray binaries (Corbet 1986; Waters & van Kerkwijk 1989), and the inferred mass function range is also consistent with this classification. Unlike GRO J1948+32, the known Be/X-ray binary systems are typically in highly eccentric orbits ($e \gtrsim 0.3$), but this may be an observational selection effect. The system has some similarities to the 12.3 s transient X-ray pulsar GS 0834−430, which has a wide, mildly eccentric ($e = 0.128 \pm 0.063$), 112 day orbit with a small mass function (Wilson et al. 1994). Both systems exhibit transient outbursts which last for a large fraction of the orbital period, but both systems also go for multiple orbital cycles without any detectable emission. (BATSE has observed only one outburst from GRO J1948+32 despite greater than 18 orbital cycles of the pulsar since the launch of *GRO*.)

We thank the referee, Ocker C. de Jager, for a careful reading of the manuscript and I. Neill Reid for arranging a Palomar Schmidt plate observation of the region during the outburst. John Chiu developed many of the BATSE spectral fitting tools used at Caltech. This work was funded in part by NASA grant NAG 5-1458. D. C. was supported by a NASA GSRP Fellowship, grant NGT-51184. L. B. was supported by Caltech's Lee A. DuBridge Fellowship, funded by the Weingart Foundation; and by a NASA Compton Fellowship, grant NAG 5-2666.

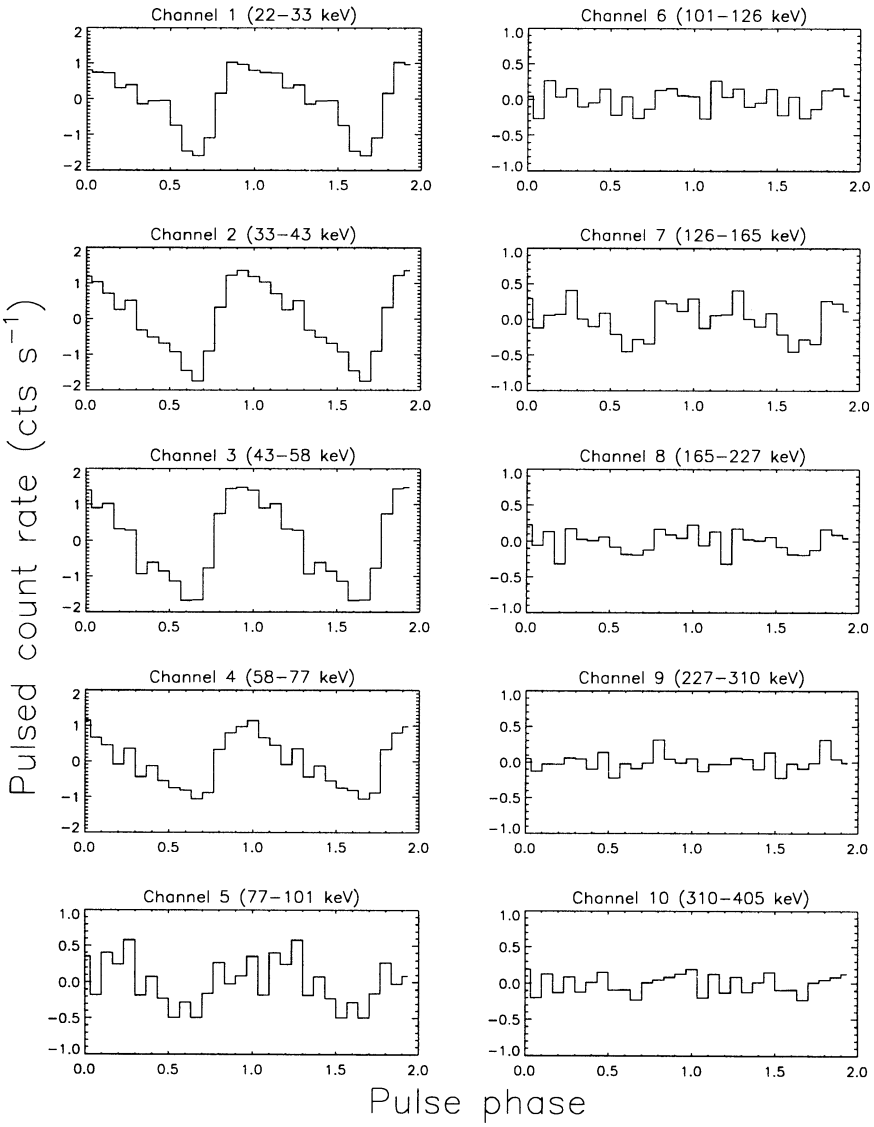

FIG. 3.—Pulse profiles as a function of energy for GRO J1948+32, during the interval MJD 49462–49468. Two pulses are shown for each channel. The energy edges for each CONT channel of BATSE detector 0 are indicated. These pulse profiles are overresolved by a factor of 1.7. Note that the pulse shapes are uncorrected for the rapid change in detector response as a function of energy in the 20–100 keV range.

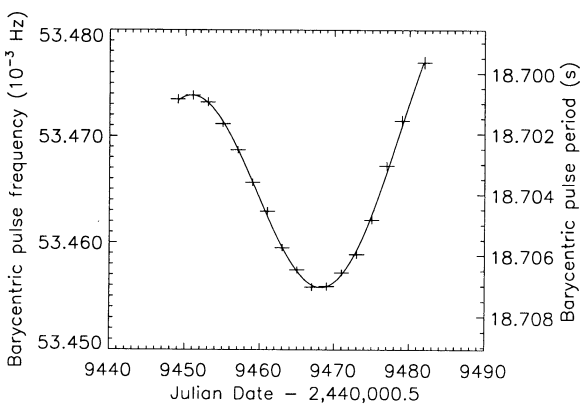

FIG. 4.—Pulse frequency history of GRO J1948+32 from BATSE observations. The vertical bars show the 1 σ statistical uncertainties in the frequency measurements, while the horizontal bars show the time interval over which each measurement was integrated. A wide range of orbital parameters can produce a nearly identical model curve (*solid curve*).

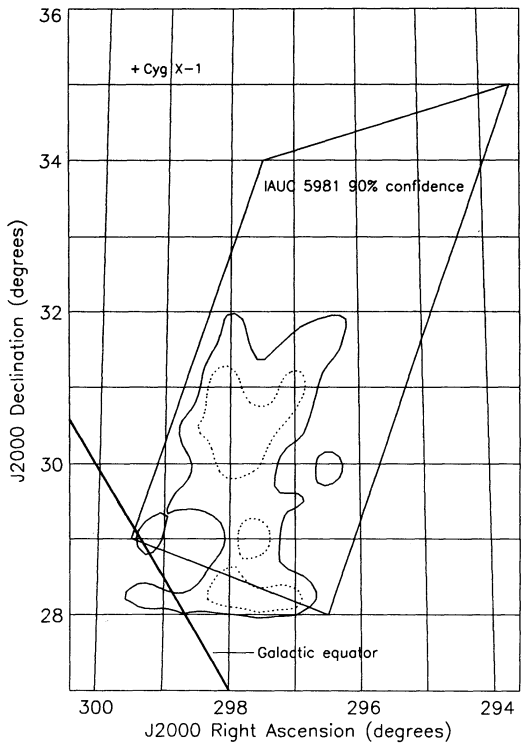

FIG. 5.—Position estimate for GRO J1948+32 ($l \sim 65°$, $b \sim 2°$). The broken contours show the formal 90% confidence region, while the solid contours show the formal 99% confidence region. These contours do not include the systematic uncertainty (see text). For comparison, the large quadrilateral is the earlier 90% confidence estimate by Chakrabarty et al. (1994).

APPENDIX

BATSE LOCALIZATION OF FAINT PULSED SOURCES

BATSE can localize intense transient sources (e.g., gamma-ray bursts) to within $\approx 5°$ accuracy by using the ratios of measured intensities in the various incident detectors (Brock et al. 1992; Fishman et al. 1994). Bright persistent sources are localized more precisely ($\sim 0.^\circ 1$) using Earth occultation edge measurements (Harmon et al. 1993; Zhang et al. 1994). Neither of these techniques is directly applicable to sources like GRO J1948+32 which are too faint ($\lesssim 100$ mCrab) to localize using standard occultation edge techniques, even though their pulsed flux is detectable by integrating the data over some interval. For such sources, it is still possible to extract spatial information from Earth occultations by using them to define the time intervals over which the pulsed signal is integrated. The maximum Fourier power is used to determine the maximum-likelihood sky location, subject to the assumptions discussed below.

To avoid complications due to uncertainties of the angular response calibration of the different detectors, we will restrict ourselves to data from the single BATSE detector with the most favorable viewing angle to the source. For an assumed sky position (α, δ) and pulse frequency ν_0, we first construct a sinusoidal model time series

$$M_j(A, \phi, \alpha, \delta) = A \cos(2\pi\nu_0 t_j + \phi) W_j(\alpha, \delta) , \tag{A1}$$

where A and ϕ are the amplitude and phase of the sinusoid, and $W_j(\alpha, \delta)$ is a visibility window function whose value is taken to be zero or unity depending upon the assumed source location and the spacecraft position with respect to the Earth. If we assume Gaussian statistics for the observed data, then the probability of model $\{M_j\}$ given an observed time series $\{S_j\}$ is

$$\Pr = \prod_{j=1}^{N} \frac{e^{-(S_j - M_j)^2/2\sigma^2}}{\sqrt{2\pi\sigma^2}} , \tag{A2}$$

where σ is the standard deviation of the background noise level, assumed to be constant over the integration. We can then write the likelihood function

$$L = 2 \ln \Pr = -\frac{1}{\sigma^2} \sum_{j=1}^{N} (S_j - M_j)^2 + \text{constant} \tag{A3}$$

$$= \frac{2A}{\sigma^2} \sum_{j=1}^{N} S_j W_j \cos(2\pi\nu_0 t_j + \phi) - \frac{A^2}{\sigma^2} \sum_{j=1}^{N} W_j^2 \cos^2(2\pi\nu_0 t_j + \phi) , \tag{A4}$$

where we have dropped the constant terms. Defining the duty fraction $\epsilon \equiv \Sigma W_j^2/N = \Sigma W_j/N$ and the trial time series $Q_j = S_j W_j$, equation (A4) becomes

$$L = \frac{2A}{\sigma^2} \sum_{j=1}^{N} Q_j e^{2\pi i \nu_0 t_j + i\phi} - \frac{A^2}{2\sigma^2} \sum_{j=1}^{N} W_j e^{4\pi i \nu_0 t_j + 2i\phi} - \frac{\epsilon N A^2}{2\sigma^2} \tag{A5}$$

$$= \frac{2A}{\sigma^2} \tilde{Q}_k e^{i\phi} - \frac{A^2}{2\sigma^2} \tilde{W}_{2k} e^{2i\phi} - \frac{\epsilon N A^2}{2\sigma^2}, \tag{A6}$$

where $\tilde{Q}$ and $\tilde{W}$ are the discrete Fourier transforms of Q and W, respectively, and k is the frequency index corresponding to ν_0. Since $\tilde{W}$ is dominated by harmonics of the spacecraft orbital frequency $\nu_{GRO} \ll 2\nu_0$ (where $1/\nu_{GRO} \approx 93$ minutes), we can generally assume $|\tilde{W}_{2k}| \ll \epsilon N$ and neglect the second term in equation (A6).

For a given sky position (α, δ), the maximum-likelihood value is obtained by maximizing L with respect to A, ϕ, and ν_0,

$$L_{opt}(\alpha, \delta) = \frac{2|\tilde{Q}_k|^2}{\epsilon N \sigma^2} = 2P_k(\alpha, \delta), \tag{A7}$$

where $P_k = |\tilde{Q}_k|^2/\epsilon N \sigma^2$ is the unity-normalized Fourier power at frequency ν_0. (The factor of ϵ in the denominator of this definition appears because a fraction $1 - \epsilon$ of the time series $\{Q_j\}$ has been set to zero.) If we define L_{opt} as the maximum value of L found by varying all five parameters (A, ϕ, ν_0, α, δ) and define L_{true} as the maximum value of L found by varying only A, ϕ, and ν_0 but holding α and δ fixed at the (unknown) true coordinates of the source, then Cash (1979) has shown that the likelihood ratio statistic

$$\Delta L = L_{opt} - L_{true} \tag{A8}$$

$$= 2P_{opt} - 2P_{true} \tag{A9}$$

$$= 2\Delta P \tag{A10}$$

is distributed as a χ^2 variable with two degrees of freedom, where we have assumed that the optimum and true coordinates are within $\sim 10°$ of each other so that $\epsilon_{true} \approx \epsilon_{opt} \approx \epsilon$.

We now estimate the celestial coordinates of a periodic pulsed source of known frequency by computing L for a grid of trial positions (α, δ). The maximum-likelihood estimate for the source position is the grid point with the optimum L value. Confidence intervals can be constructed using contours of $\Delta\chi_2^2 = \Delta L = L_{opt} - L$. A 90% confidence region corresponds to a contour of $\Delta\chi_2^2 = 4.6$ while a 99% confidence region corresponds to a contour of $\Delta\chi_2^2 = 9.2$ (Lampton, Margon, & Bowyer 1976). Multiple time series can be treated in the same way. Each time series contributes an additional product series in equation (A2), or equivalently additional terms in equation (A7). Thus, despite a larger aggregate value of L, the ratio statistic ΔL will still be distributed as χ_2^2.

This method implicitly assumes a constant sinusoidal signal and a constant Gaussian background over the entire interval of interest. Since real data depart from this idealization, we expect that systematic errors will eventually limit the precision of the technique. To estimate this limit, we studied DISCLA data from the recent bright outburst of the 3.6 s accreting pulsar 4U 0115+63 (Wilson, Finger, & Scott 1994). For the 20–60 keV channel, the background level varied between 1000 and 2000 counts s^{-1} over the spacecraft orbit. Using a location grid spacing of 0°.25 and 25 days of data, our estimated 99% confidence region was $\approx 1°$ across, centered on the true position of the source (which is known to within several arcseconds from optical astrometry of the companion). Given the strength of the signal in these data, we will adopt 0°.5 as the systematic precision limit of this technique with DISCLA data.

REFERENCES

Brock, M. N., Meegan, C. A., Roberts, F. E., Fishman, G. J., Wilson, R. B., Paciesas, W. S., & Pendleton, G. N. 1992, in Gamma-Ray Bursts, ed. W. S. Paciesas & G. J. Fishman (New York: AIP Press), 383

Cash, W. 1979, ApJ, 228, 939

Chakrabarty, D., et al. 1993, ApJ, 403, L33

Chakrabarty, D., Prince, T. A., Finger, M. H., Wilson, R. B., & Pendleton, G. N. 1994, IAU Circ., No. 5981

Corbet, R. H. D. 1986, MNRAS, 220, 1047

de Jager, O. C. 1994, ApJ, 436, 239

Finger, M. H., Stollberg, M., Pendleton, G. N., Wilson, R. B., Chakrabarty, D., Chiu, J., & Prince, T. A. 1994, IAU Circ., No. 5977

Fishman, G. J., et al. 1989, in Proc. of the GRO Science Workshop, ed. W. N. Johnson (Greenbelt: NASA/GSFC), 2–39

Fishman, G. J., et al. 1994, ApJS, 92, 229

Giacconi, R., Gursky, H., Kellogg, E. M., Schreier, E., & Tananbaum, H. 1971, ApJ, 167, L67

Goodman, J. W. 1985, Statistical Optics (New York: Wiley)

Harmon, B. A., et al. 1993, in Compton Gamma-Ray Observatory, ed. M. Friedlander, N. Gehrels, & D. J. Macomb (New York: AIP Press), 314

Heindl, W. A., Cook, W. R., Grunsfeld, J. M., Palmer, D. M., Prince, T. A., Schindler, S. M., & Stone, E. C. 1993, ApJ, 408, 507

Kahabka, P., et al. 1994, A&A, in preparation

Lampton, M., Margon, B., & Bowyer, S. 1976, ApJ, 208, 177

Nagase, F. 1989, PASJ, 41, 1

Prince, T. A., Bildsten, L., Chakrabarty, D., Wilson, R. B., & Finger, M. H. 1994, in Evolution of X-Ray Binaries, ed. S. S. Holt & C. S. Day (New York: AIP Press), 235

Reid, I. N., et al. 1990, PASP, 103, 661

Rubin, B. C., et al. 1993, in Compton Gamma-Ray Observatory, ed. M. Friedlander, N. Gehrels, & D. J. Macomb (New York: AIP Press), 1127

Waters, L. B. F. M., & van Kerkwijk, M. H. 1989, A&A, 223, 196

Wilson, C. A., Harmon, B. A., Wilson, R. B., Fishman, G. J., & Finger, M. H. 1994, in Evolution of X-Ray Binaries, ed. S. S. Holt & C. S. Day (New York: AIP Press), 259

Wilson, R. B., Finger, M. H., & Scott, D. M. 1994, IAU Circ., No. 5999

Zhang, S. N., Fishman, G. J., Harmon, B. A., & Paciesas, W. S. 1994, Nature, 366, 245